REEXAMINATION OF THE DOUBLE SUCROSE GAP TECHNIQUE FOR THE STUDY OF LOBSTER GIANT AXONS

Theory and Experiments

JOHN P. POOLER AND DENNIS P. VALENZENO
Department of Physiology, Emory University School of Medicine, Atlanta, Georgia 30322

ABSTRACT The double sucrose gap technique for the study of lobster giant axons has been reexamined. The leakage behavior of the system cannot be successfully modeled by conventional sucrose gap theory, but is accounted for by the McGuigan-Tsien model that takes into account the cable properties of membrane under sucrose. The facts of high-leakage conductance and the ability to maintain large resting potentials in the face of low sucrose gap resistance lead to a hypothesis that membrane resistance under sucrose is very low because of a large negative surface potential. Computer simulations of the leakage behavior of the conventional gap model and the McGuigan-Tsien model were compared with experimental measurements on lobster axons using normal sucrose or sucrose doped with Na^+, Ca^{2+} or La^{3+} ions. As the concentration of doping ion increased, the leakage rose, but the species of doping ion had more influence on leakage than gap resistance. At equal gap resistance, leakage decreased with an increase in valence of the doping species. Leakage was even lower in La-doped sucrose at 20 MΩ gap resistance than in normal sucrose at 200 MΩ gap resistance. Resting potentials decreased with decreasing gap resistance and increasing valence of the doping species. Resting potential behavior was successfully simulated with a hybrid model consisting of a point node flanked by infinite cables and a shunt between ground and the voltage-measuring pool. The data support the hypothesis that the membrane resistance under sucrose is low and that it can be raised by doping the sucrose with multivalent cations, with La^{3+} being particularly effective. Both the leak conductance and resting potential are influenced more by membrane under sucrose than membrane in the node. The experiments also demonstrate that doping with La^{3+} vastly improves the stability and longevity properties of the lobster axon preparation.

INTRODUCTION

The sucrose gap technique for assessing membrane potentials of nerve axons with extracellular electrodes was first reported by Stampfli (1954) and extended for purposes of voltage clamping giant axons by Julian et al. (1962 *a*, *b*). The technique is particularly useful for measuring pharmacological modifications of channel properties that are irreversible or where there is large scatter in the degree of change, since sequential pulling of untreated regions of membrane into the node between the sucrose regions permits a number of independent determinations to be made from just one axon. The sucrose gap technique has also seen widespread application to multicellular muscle tissue (reviewed by Beeler and McGuigan, 1978).

The lobster axon sucrose gap system has several anomalous properties not in keeping with the original theory that have never been explained. First, the leakage is much higher than expected on the basis of membrane properties. From Brinley's (1965) measurements of resting membrane resistance using microelectrodes, which averaged over 8,000 Ωcm^2, one predicts a leakage conductance for small voltage clamped depolarizations away from a hyperpolarized holding potential to be $<<$ 1 mS cm^{-2}; yet, measured values are close to 20 mS cm^{-2} (Pooler and Oxford, 1972). Then Pooler and Oxford (1972) showed that measured leakage current in voltage clamp is independent of the node area between the sucrose streams, meaning that the majority of the current flows in parallel with the node membrane rather than through it. Following the suggestion of New and Trautwein (1972) that doping the sucrose solution with calcium improved muscle preparation viability, Oxford and Pooler (1975) used a calcium doping procedure on giant axons for the same purpose. Surprisingly, the resulting lowering of gap resistance did not short-circuit the resting potential. Typical node dimensions and Brinley's (1965) value for membrane resistance give a predicted node membrane resistance of 35 MΩ. The calcium doping procedure lowered gap resistance to 10 MΩ, which

Dr. Valenzeno's present address is Department of Physiology, University of Kansas Medical Center, Kansas City, KS 66103

should have short-circuited the preparation. It was obvious that the membrane under the sucrose was contributing to the observed properties and that a theory that took account of the cable properties in the sucrose regions was needed. Jirounek and Straub (1971) developed a model for the measured resting potential but it contained too many unmeasurable quantities to be tested experimentally. Then McGuigan and Tsien (1974) derived a theoretical model for the leak conductance that contained only one unmeasurable quantity, the resistance of the membrane in the sucrose region. They performed calculations based on the assumption that this resistance was the same as that in the node region, but the model permits any value to be used. In the present work predictions of sucrose gap properties based on the McGuigan-Tsien model are compared with those of the conventional model, and both are compared with experimental measurements.

For theoretical reasons, it seems likely that the membrane resistance in the sucrose region should be considerably lower than in the node region. First, membranes tend to deteriorate in calcium-free solutions (Muir, 1967). Second, the lack of binding of calcium by the membrane and the low ionic strength of sucrose both ought to increase the magnitude of the negative surface potential and, thereby, shift the current-voltage relation for potassium in the direction of more negative membrane potentials. This, in turn, will raise the potassium permeability and decrease membrane resistance relative to the node region for any given level of membrane potential.

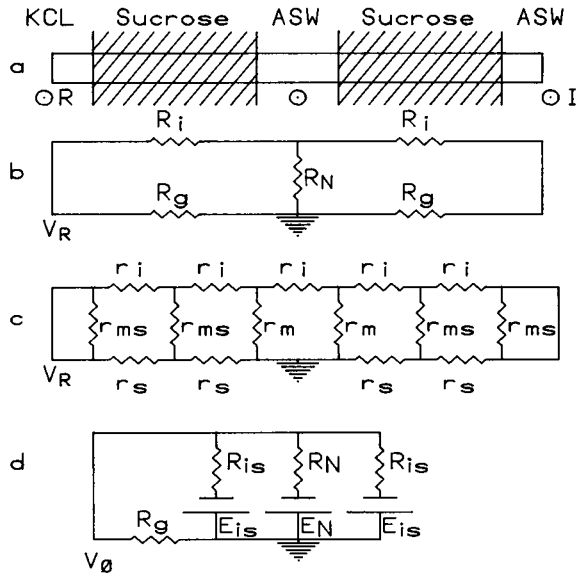

FIGURE 1 Double sucrose gap. (*a*) The axon is bathed in five pools with electrodes as shown. The KCl pool contains 0.5 M KCl. The central and *I* pools contain artificial sea water. (*b*) Leakage properties of the system according to conventional theory. The membrane resistance in the side pools is approximated by a zero value because the area available for current flow is unlimited. (*c*) Leakage properties of the system according to the McGuigan-Tsien model. (*d*) Hybrid model of resting potential. All symbols are defined in the text.

If the foregoing reasoning is valid, it should be possible to manipulate the membrane resistance in the sucrose region by selective doping of the sucrose with ions. In the present work different concentrations and species of doping ions have been used to raise the membrane resistance back toward the level found in the node region. This procedure has the complication of lowering the sucrose resistance, however, and one has to separate effects due to a putative raising of membrane resistance from effects due to a lowering of sucrose resistance. To accomplish this, the doping solutions were matched for resistance, so that different species of doping ion could be used at equivalent gap resistance. Specifically, Na^+, Ca^{2+}, and La^{3+} were used as doping ions at concentrations chosen to yield equivalent gap resistance. From a consideration of the effects of these ions on voltage-dependent conductances on lobster axons (Julian et al., 1962 *b*, Blaustein and Goldman, 1968; Takata et al., 1966) and from their ability to modify surface potentials (McLaughlin et al., 1971), the predicted order of effectiveness in raising membrane resistance is $Na^+ < Ca^{2+} < La^{3+}$. The results show that the properties of the sucrose gap can be accounted for by the McGuigan-Tsien theory, modified by the surface charge considerations described above. The results also yield a very practical finding. Doping the sucrose with La^{3+} vastly improves the stability and rundown properties of the system without any obvious pharmacological effect on Na and K voltage-sensitive conductances.

THEORY

Fig. 1 *a* depicts the main physical elements of an axon in double sucrose gap. There are five solutions flowing across the axon, with electrodes in the outside and middle solutions. The middle electrode is connected to the virtual ground of a current to voltage transducing amplifier. The R (recording) electrode is connected to the high-impedance input of an isolation amplifier that feeds the signal back to the clamp amplifier while the I (current injection) electrode is connected to the output of the clamp amplifier. The gap leak is defined as I/V_R, where I (in amperes) is the change in current flowing into the virtual ground electrode from the I electrode and V_R (in volts) is the change in potential of the R electrode when the potential is step changed under voltage clamp conditions.

Fig. 1 *b* models the leakage properties of the system according to conventional sucrose gap theory (omitting sources of resting potential). R_g, R_i, and R_N represent resistance (in ohms) of the sucrose gap, longitudinal intracellular medium, and the membrane of the node, respectively. The gap leak given by Eq. 1 is derived in a straightforward manner by summing the currents between the I and virtual ground electrode, and dividing this by V_R:

$$G_L = (R_G + R_i)(2R_N + R_G + R_i)/(R_N R_G^2). \quad (1)$$

R_i is related to the intracellular resistivity ρ_i (Ωcm), gap width w (cm), and axon diameter D (cm) by Eq. 2,

$$R_i = 4\rho_i w/\pi D^2, \quad (2)$$

while R_N is related to the membrane resistance R_m (Ωcm^2), node length l (cm), and D by Eq. 3.

$$R_N = R_m/\pi Dl. \quad (3)$$

Fig. 1 *c* models the leakage properties according to the McGuigan-Tsien theory, where r_s and r_i are longitudinal resistances per unit length (Ωcm^{-1}) of the sucrose and intracellular medium, and r_m and r_{ms} are the membrane resistances per unit length (Ωcm) of the node and sucrose regions.

The expression for gap leak using the McGuigan-Tsien theory is obtained by combining their Eqs. 2 and 15 to give Eq. 4;

$$G_L = [(r_s + r_i)/r_s]^2[1/(\lambda r_i)]$$
$$[\sinh L + B\cosh L + B(\cosh L + B\sinh L)]. \quad (4)$$

The expressions for λ, L, B, r_i, r_m, r_{ms} and r_s are given by Eqs. 5–11, where R_{ms} (Ωcm^2) is the membrane resistance under sucrose.

$$\lambda = (R_m D/4\rho_i)^{1/2} \quad (5)$$

$$L = l/\lambda \quad (6)$$

$$B = \{r_m r_i/[r_{ms}(r_s + r_i)]\}^{1/2} \quad (7)$$

$$r_i = 4\rho_i/\pi D^2 \quad (8)$$

$$r_m = R_m/\pi D \quad (9)$$

$$r_{ms} = R_{ms}/\pi D \quad (10)$$

$$r_s = R_g/w. \quad (11)$$

A cable model for the resting potential is much more complex. A simplified approximation is a hybrid model in which a point node is flanked on each side by half of an infinite cable. With one side pool depolarized in KCl, the finite gap resistance shunt must be included to give the circuit analog shown in Fig. 1 *d*. The measured resting potential (V_o) is given by Eq. 12, where E_N and E_{ms} are the zero current potentials of the node and membrane under sucrose, and R_{is} is the standard input resistance of each half cable, as given in Eq. 13

$$V_o = (E_n R_{is} + 2E_{ms}R_N)R_g/(2R_gR_N + R_gR_{is} + R_NR_{is}) \quad (12)$$

$$R_{is} = [r_{ms}(r_i + r_s)]^{1/2}. \quad (13)$$

R_{is} appears as a single element, but it subsumes intracellular, extracellular and membrane resistance. Note that R_g appears both as a discrete element and as part of R_{is}.

Calculations

Calculations of gap leak or resting potential as a function of a given parameter used the following standard values for the nonvaried parameters. R_m = 8,000 Ωcm^2; R_{ms} = 8,000 Ωcm^2; ρ_i = 30 Ωcm; D = 0.01 cm; l = 0.0075 cm; w = 0.105 cm; R_g = 2×10^8 Ω. The use of values different from these is noted in the figures.

MATERIALS AND METHODS

The sucrose gap chamber is similar in principle and basic design to that illustrated in Julian et al. (1962 *a*). The two side pools are open slots milled out of a block of Lucite. The two sucrose pools are formed by a horizontal hole drilled through solid Lucite from one side pool to the other through which the axon is threaded. This hole is intersected at right angles by a second hole, which forms the central pool. Central pool solutions flow from back to front across the axon while sucrose flows upward on either side of the central pool into the lateral hole to form the two sucrose gaps. The lateral hole is 0.313 mm in diameter, and the length from each side pool to the central pool is 1.05 mm. Measured gap resistances agree quite well with calculations based on these dimensions and measured solution resistivity. The solutions bathing the central pool and current injection pool contained an artificial sea water (ASW) with

TABLE I
COMPOSITION OF SUCROSE SOLUTIONS

Name	Doping species	Concentration	Resistivity	Gap resistance
		M	Ωcm	Ω
Na 5	NaCl	4.2×10^{-4}	3.3×10^4	5×10^6
Na 10	NaCl	2.1×10^{-4}	6.5×10^4	10×10^6
Na 20	NaCl	1.1×10^{-4}	1.3×10^5	20×10^6
Ca 5	$CaCl_2$	2×10^{-4}	3.3×10^4	5×10^6
Ca 10	$CaCl_2$	1×10^{-4}	6.5×10^4	10×10^6
Ca 20	$CaCl_2$	5×10^{-5}	1.3×10^5	20×10^6
La 5	$LaCl_3$	1.3×10^{-4}	3.3×10^4	5×10^6
La 10	$LaCl_3$	6.7×10^{-5}	6.5×10^4	10×10^6
La 20	$LaCl_3$	3.4×10^{-5}	1.3×10^5	20×10^6

All solutions contained 0.725 M sucrose. Resistivities varied ± 10% and gap resistances ± 20% from the values shown.

acetate as the predominant anion. The use of acetate eliminates the hyperpolarizing effect of choloride-rich solutions (Blaustein and Goldman, 1966). The concentrations were Na acetate, 471 mM; Ca acetate$_2$, 25 mM; K acetate, 10 mM; HEPES, 4 mM titrated to pH 7.6 at 4°C. The sucrose solutions, 725 mM, were made by dissolving sucrose in deionized water and then deionizing the solution in a Deeminite ion exchange resin (Crystalab, Inc. Hartford, CT) to yield a resistivity of ~1.5×10^6 Ωcm as measured with a Beckman RC 16B2 conductivity bridge (Beckman Instruments, Inc., Palo Alto, CA). The sucrose was then doped by addition of concentrated NaCl, $CaCl_2$ or $LaCl_3$. Sucrose solutions are identified by the doping cation and gap resistance. For example, Na 5 means a sucrose solution doped with NaCl to yield a gap resistance of 5 MΩ. Table I shows the composition of the solutions used.

The medial giant axon from the circumesophageal connective nerve of lobster (*Homarus americanus*) was dissected in chilled ASW under dark-field illumination and transferred immediately to the sucrose gap chamber without passing through an air-water interface.

Switching between sucrose solutions was not instantaneous because of unavoidable dead space. Upon switching to a new solution with a different conductivity, the measured gap conductance rose or fell after a 30 s delay with a time constant of 40–50 s, meaning that better than 95% replacement occurred within 3 min and better than 99% within 5 min.

Raw data were recorded on a Nicolet Explorer III digital oscilloscope (Nicolet Instrument Corp., Madison, WI) and transferred for analysis to a Tektronix 4052 computer (Tektronix, Inc., Beaverton, OR). To measure gap leak, the potential was clamped to −100 mV and step depolarized by 30 mV. The ratio of change in current to change in potential was assessed 4 ms after the change in potential. Data were recorded at 1 min intervals beginning with the first minute after forming a new node.

RESULTS

Undoped Sucrose

Measurements and Predictions. The gap leak in undoped sucrose averaged 0.635 μS (median 0.588 μS). The individual values for 14 determinations are shown in Fig. 2 along with calculated values plotted as a function of R_{ms}, the membrane resistance under sucrose. The dotted curve in Fig. 2 is the gap leak predicted by conventional gap theory (Eq. 1) while the solid curve is the prediction of the McGuigan-Tsien model (Eq. 4). Even the lowest measured leak value was considerably larger than the conventional theory predicts, a result already expected

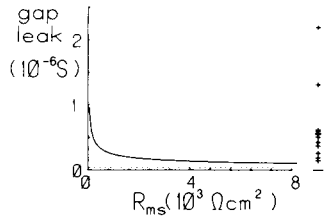

FIGURE 2 Individual values of gap leak in normal sucrose (+) and calculated gap leak vs. R_{ms}. The dotted curve (···) is calculated according to the conventional model (Eq. 1), while the solid curve (—) is calculated according to the McGuigan-Tsien model (Eq. 4).

from the anomalies of the system described in the introduction. For all values of R_{ms} the McGuigan-Tsien theory predicts a larger leak than the conventional theory, and if R_{ms} is set to 234 Ωcm^2 the prediction matches the experimentally measured value. The fact that model predictions can only be made to match measured leak by decreasing R_{ms} is consistent with the hypothesis that R_{ms} in undoped sucrose is much lower than R_m.

Fig. 3 compares the predictions of the conventional model and McGuigan-Tsien model for gap leak as a function of several other parameters, using a value of 234 Ωcm^2 for R_{ms}. Both models predict gap leak to be virtually independent of internal resistivity, ρ_i (Fig. 3 *a*). The two models give rather different predictions about the dependence on node width (Fig. 3 *b*). The conventional model predicts a direct proportionality between leak and node width while the McGuigan-Tsien model predicts relatively little dependence. Pooler and Oxford (1972) have shown experimentally that gap leak does not vary with node width in undoped sucrose. Gap leak is predicted to vary with axon diameter by both models (Fig. 3 *c*), but axon diameters tend to cluster near 100 μm in adult lobsters (Govind and Lang, 1976) and variations in diameter are probably not a major contributor to variations in measured leak. Both models predict that leak should rise as R_m decreases (Fig. 3 *d*) although the McGuigan-Tsien predicition is quite flat until R_m drops below ~2,000 Ωcm^2, a value much lower than the lowest value for R_m measured by Brinley (1965) of 4,095 Ωcm^2.

These calculations indicate that two of the anomalies of the sucrose gap, a leak much higher than expected from node membrane characteristics and a leak independent of node width, are successfully accounted for by the McGuigan-Tsien model, modified by a hypothesis of a low R_{ms}. The conventional model fails to predict these properties. A

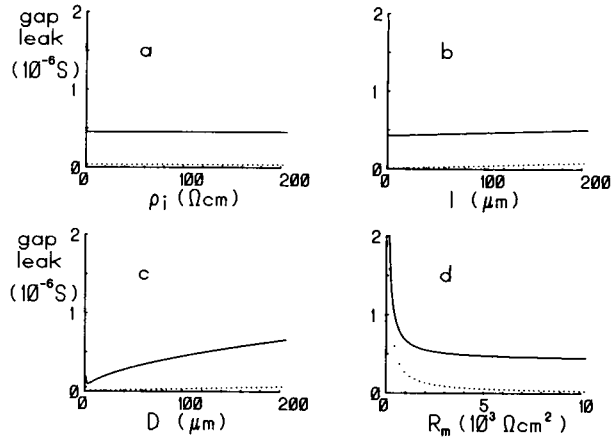

FIGURE 3 Calculated gap leak according to conventional model (· · ·) and the McGuigan-Tsien model (—). (*a*) G_L vs. ρ_i. (*b*) G_L vs. *l*. (*c*) G_L vs. *D*. (*d*) G_L vs. R_m. In the calculations, the values for the nonvaried parameter are those given in the text but with R_{ms} set to 234 Ωcm^2.

sterner test of the hypothesis comes from experiments in which the sucrose resistance is lowered by doping with ions.

Doped Sucrose

Measurements and Predictions. In the following set of experiments, the sucrose was switched at 5 min intervals between different concentrations of a given doping ion. Separate axons were used for each doping species. Measurements of gap leak were taken after 5 min in a given solution, just before switching to the next. The results are presented in Table II and Fig. 4. Quite clearly gap leak depends on both the species of doping ion and the gap resistance. Leak was lowest in La and highest in Na, and, for a given species, rose as gap resistance fell. In La 20 the leak was even lower than in undoped sucrose. The species of doping ion had much more influence on gap leak than did the gap resistance. These trends are easiest to see in Fig. 4 where the mean leak values are plotted along with calculations. The measured leak values in Na-doped sucrose are undoubtedly biased in the low direction. Most axons did not tolerate Na-doped sucrose very well, particularly Na 5, and a number of runs that would have yielded high leak values did not survive the 5 min needed to make the measurement. In contrast, the axons were quite stable in Ca and La, particularly La, as described further on.

Fig. 4 also shows a family of calculated gap leak curves as a function of R_g. The data for La-doped sucrose

TABLE II
GAP LEAK (μS) IN DOPED AND NORMAL SUCROSE

	Normal	Na 5	Na 10	Na 20	Ca 5	Ca 10	Ca 20	La 5	La 10	La 20
mean	0.64	1.75	1.68	1.56	1.56	1.12	0.98	0.86	0.63	0.47
SD	0.53	0.43	0.94	0.90	0.64	0.39	0.40	0.21	0.20	0.14
n	14	13	11	11	21	25	21	21	20	21

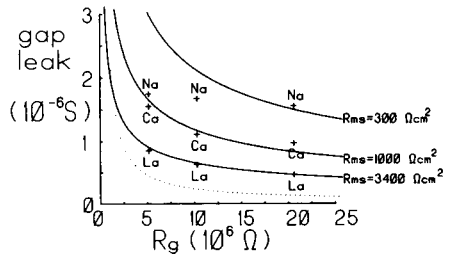

FIGURE 4 Mean values of gap leak from Table II (+) vs. R_g, and calculations according to the conventional model (···) and the McGuigan-Tsien model (—).

coincided reasonably well with calculated leak using an R_{ms} of 3,400 Ωcm². The measured leak in Ca-doped sucrose was higher than in La-doped sucrose, and the calculated curve with an R_{ms} of 1,000 Ωcm² is a reasonable fit. In Na-doped sucrose the leak was higher yet, but the previously mentioned caveat about the Na data precludes drawing any conclusions about the fit. Qualitatively, at least, these data are consistent with the hypothesis that the membrane resistance under sucrose is low and that it is progressively increased by doping the sucrose with ions that are progressively more effective in reducing the surface potential.

Switching Between La-doped and Na-doped Sucrose

Experiments were also carried out where the sucrose was switched between La 10 and Na 10, solutions of equal gap resistance. After 5 min in one solution the leak was measured and the input was switched to the other solution. After 5 min in the second solution the leak was measured again. The ratios of the second to the first determination are given in Table III. As expected from the earlier results, the leak dropped upon switching to La 10 sucrose and rose upon switching to Na 10. Quantitatively, these differences are not as large as found when separate axons were used for each doping species. The reason is that the leak-lowering action of La is only partly reversible. Once the membrane had been exposed to La the leak usually remained at a low level, even upon switching back to Na-doped sucrose.

TABLE III
CHANGES IN GAP LEAK UPON SWITCHING TO A NEW SUCROSE SOLUTION

	From Na 10 to La 10	From La 10 to Na 10
mean	0.85	1.127
SD	0.085	0.164
n	18	13

Values are mean ratios of gap leak in the second solution relative to the first, as explained in the text.

Resting Potentials in Doped Sucrose

One of the main reasons for questioning the legitimacy of conventional sucrose gap theory is that resting potentials are not short-circuited by doped sucrose. According to conventional theory an R_g of 5 MΩ ought to reduce the measured resting potential to less than −10 mV, yet values in the −60 to −80 mV range are commonly observed. If the cable properties of membrane under sucrose contribute to leakage current, they should also influence the measured potential when the preparation is not voltage clamped. The degree of this influence should vary with both R_{ms} and R_g, as predicted by Eq. 12.

These predictions were tested by recording the changes in resting potential as the sucrose solutions were switched at 5 min intervals. A factor that complicates the measurements is spontaneous drift in resting potential. To compensate for drift, a linear regression analysis was performed on the resting potential values for the 3 min prior to switching to a new solution. The drift was extrapolated ahead 5 min to form an expected value and then compared with the measured value. The data entries consist of measured potential 5 min after switching minus the expected values. To illustrate, if the resting potential were spontaneously depolarizing at the rate of 0.5 mV/min and the potential just before switching were −60 mV, the expected value 5 min later would be −57.5 mV. If the measured value were actually −65 mV then the recorded change would be −7.5

TABLE IV
EFFECT OF CHANGES IN SUCROSE DOPING IONS ON RESTING POTENTIAL

Gap resistance	Ion species				
	Na to Na	Na to La	La to Na	La to La	Ca to Ca
MΩ					
20 to 5				+4.99 ± 7.51 (4)	+8.84 ± 12.70 (5)
20 to 10	+14.94 ± 13.7 (2)			+2.97 ± 6.00 (17)	+8.97 ± 6.66 (5)
10 to 5	+16.27 ± 9.92 (3)			+2.93 ± 5.90 (16)	+11.10 ± 12.29 (13)
10 to 10	+1.86 ± 3.97 (9)	+19.27 ± 4.29 (18)	−10.96 ± 5.73 (12)		
5 to 10				−8.27 ± 2.93 (4)	−3.57 ± 3.72 (5)
10 to 20				−0.79 ± 5.07 (2)	−1.27 ± 4.69 (10)
5 to 20	−10.89 ± 9.91 (3)			−6.89 ± 5.46 (12)	−3.84 ± 8.76 (8)

Column entries are mean change in resting potential [± SD (*n*)] upon switching to a new solution, as defined in the text. Positive values indicate a depolarization, and negative entries a hyperpolarization.

mV. Data were rejected if the spontaneous drift rate exceeded 3 mV/min. The results are presented in Table IV.

Two clear trends are evident in the data. For a given doping species, switching to a lower gap resistance depolarized and switching to a higher gap resistance hyperpolarized the preparation. The other trend is that resting potentials were more depolarized in lanthanum than sodium. Switching from Na 10 to La 10 depolarized almost 20 mV even though R_g was unchanged. Return to Na 10 hyperpolarized by almost 11 mV. These effects of La and Na on resting potentials are striking in view of their influence on gap leak. La reduces gap leak, yet it depolarizes the preparation. Such a dual effect is incompatible with conventional sucrose gap theory, but makes sense if the cable properties of the sucrose region are considered and if the role of La is to increase R_{ms}.

On a given node the first switch from Na-doped to La-doped sucrose depolarized much more than subsequent switches. As noted in the data on gap leak, the influence of La was only partially reversible and this incomplete reversibility was manifested on resting potentials as well. The various behaviors described above are illustrated in Fig. 5, which is an example of raw data for gap leak and resting potential from a node where the sucrose was switched back and forth between Na 10 and La 10. Notice the substantial fall in resting potential and gap leak upon first switching to La 10 and the smaller changes thereafter.

Longevity and Stability in La-doped Sucrose

Two vexing problems with the sucrose gap technique are preparation longevity and stability. With undoped sucrose it is rare to keep a node with large inward sodium currents viable for more than 30 min. One frequently observes sudden depolarizations of resting potential correlated with a rise in leak. Even if this does not occur, the kinetics of sodium current drift over time as if the holding potential were slowly changing. This makes it difficult to make comparative measurements separated in time by more than a few minutes. The use of Ca-doped sucrose decreases the drift and delays preparation rundown somewhat, but by no means eliminates the problem. La-doped sucrose, however, seems to stabilize the preparation to a remarkable degree. In no case was it necessary to terminate an experiment due to drift or rundown if La was the sole species used to dope the sucrose. Longevity tests extending 1 h or more showed on every occasion that large inward sodium currents could be elicited throughout and that there were no abrupt changes in leak or resting potential. In contrast, with normal sucrose the majority of nodes failed before 15 min. Runs lasting more than 30 min were a true exception. The number of usable nodes obtainable from one axon using La-doped sucrose seems to be limited more by the patience of the experimenter than the axon per se. If the axon is dissected in good condition one can easily study 8 nodes for an hour each, or upwards of 30 nodes, if each experiment is short.

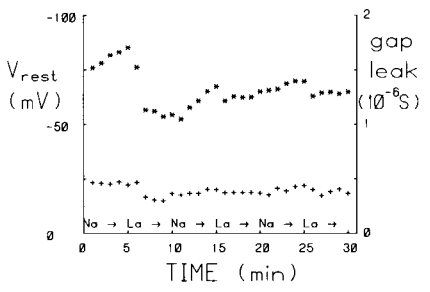

FIGURE 5 Gap leak (+) and resting potential (*) vs. time as the sucrose was switched between Na 10 and La 10 at 5 min intervals.

Fig. 6 shows a longevity test for a node with La 10 sucrose. The resting potential and peak sodium current slowly decline in a manner typical of many in vitro preparations, but the large drifts normally observed with undoped sucrose are absent. Some of the fluctuations superimposed on the general trend represent electrical noise.

DISCUSSION

Despite many years of successful application of the sucrose gap technique to giant axons from squid and lobster, it is evident the system does not work according to the principles assumed by its users. The main difference is the role played by membrane under the sucrose. Rather than being isolated from the node membrane by the high resistance of sucrose, this membrane is a key determinant of the properties of the system. All of the experiments are consistent with the hypothesis that R_{ms} is lower than R_m. Upon a small step depolarization in voltage clamp, the leakage current through node membrane is swamped by leakage through membrane under the sucrose. Therefore, the apparent specific membrane conductance is much higher than predicted from Brinley's (1965) resistance measurements, and the current for a given potential change is independent of

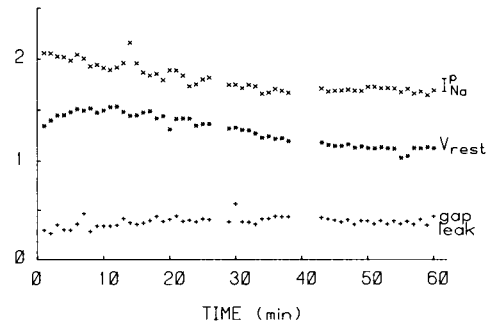

FIGURE 6 Longevity test in La-doped sucrose. Peak sodium current at −15 mV (x), resting potential (*), and gap leak (+) vs. time for a node using La 10 throughout. Each numerical division on the ordinate represents 50 mV resting potential and 1 μS gap leak. The peak sodium current is in arbitrary units.

node area. These various properties are accounted for quite well by the McGuigan-Tsien model.

The conventional model predicts leak values in the range measured here if sucrose resistance is <5 MΩ (see Fig. 4). Is it possible that leak is high because the resistance in normal sucrose with an axon in place is really much less than the 200 MΩ measured without an axon? Ions diffuse from the axon and Schwann cells, and the sleeve of unstirred solution in the periaxonal space could shunt the gap. The presence of an axon perturbs the gap resistance, lowering it by diffusion of ions, and raising it by occluding part of the cross-sectional area of the sucrose pool. The latter effect would raise gap resistance by 10–15% in the nerve chamber used here. If the effective gap resistance in undoped sucrose were really <5 MΩ then doping the sucrose with a 20 MΩ solution would add very little to the leak. The data shows that Na 20 and Ca 20 both raise gap leak considerably over normal sucrose, meaning that the effective gap resistance with an axon in place must be high relative to 20 MΩ.

According to the McGuigan-Tsien model, gap leak varies nearly inversely with the product of R_g and R_{ms}. Doping experiments are consistent with this. Increasing concentrations of doping ion lower the gap resistance and raise leakage. Even more important than sucrose resistance, however, is the species of doping ion. This fits with the McGuigan-Tsien model if different doping species differentially alter R_{ms}. When La 20 is used, the relative rise of R_{ms} is evidently greater than the drop of R_g, thereby accounting for the fact that leak in La 20 is actually lower than in normal sucrose. At higher doping concentrations, the fall in R_g exceeds the rise in R_{ms}.

Resting potential behavior in sucrose gap is rather complex. The model shown in Fig. 1 *d* offers a reasonable approximation to its properties. The zero current potential under sucrose (E_{ms}) is not known, but it is likely to be more negative than the zero current potential of the node (E_N) because the sucrose is potassium free. Blaustein and Goldman (1966) suggested a value close to −100 mV. E_N is about −71 mV (Dalton, 1958).

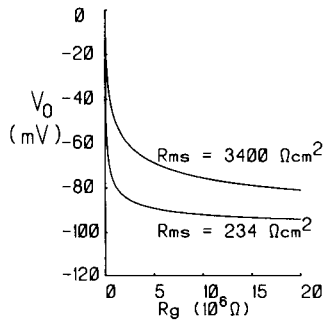

FIGURE 7 Resting potential as a function of gap resistance calculated from Eq. 12. The upper and lower curves used R_{ms} values found from leakage calculations to fit best the data in La-doped and undoped sucrose, respectively. E_N was set to −71 mV and E_{ms} to −100 mV.

Model predictions of measured resting potential using these values of E_{ms} and E_N are shown in Fig. 7. With R_{ms} set to 234 Ωcm² (the value required to match the leakage in undoped sucrose) V_o remains more negative than E_N for all gap resistances above 1 MΩ. This is consistent with observations that standard gap resistances of 10 MΩ do not short-circuit the preparation, despite the fact that the node resistance is probably close to 35 MΩ. If R_{ms} is raised to 3,400 Ωcm², however, then short-circuiting becomes more significant. The data of Table IV are consistent with these model predictions. When R_{ms} was manipulated at constant gap resistance by switching between La 10 and Na 10, the measured potentials were alway significantly more depolarized in La 10, in agreement with the idea that La raises R_{ms}. The lowering of gap resistance within a given doping species had a depolarizing influence, again in agreement with model predictions.

Resting potentials in sucrose gap tend to drift even when external conditions are constant. This is not surprising if the resting potential is influenced more by the membrane under sucrose than by the node membrane itself. Several factors contribute to drift. First, it is well known that membranes in calcium-free environments slowly change properties over time (Adelman, 1956; Huxley, 1959). Second, if the hypothesis presented here is correct, then many potassium channels, sensing a small electric field due to a large negative surface potential, would be open at rest and the membrane potential would tend toward the potassium equilibrium potential. However, with a potassium-free sucrose the effective potassium concentration in the unstirred layer in the periaxonal space would be low and subject to fluctuations associated with changing membrane properties and events in the Schwann cell layer. Third, calcium-free solutions lead to loss of intracellular potassium (Crevey et al., 1978), further contributing to changes in the potassium equilibrium potential. Therefore the measured resting potential would change slowly over time.

Julian et al. (1962 *a*) reported that axoplasm resistivity (ρ_i) rose over time, presumably due to loss of axoplasmic ions. Increasing R_{ms} by doping the sucrose should reduce this loss. Whether a rise in ρ_i has a significant influence on the behavior of the system is not clear. The model predictions shown in Fig. 3 *a* indicate that leak is not sensitive to ρ_i. It would take an enormous fractional increase to change gap leak. In model predictions of resting potential the internal and external longitudinal resistances appear as a sum and more than a 200-fold increase in ρ_i would be necessary for the internal resistance to approach the external resistance.

When the normal ASW bathing the node and current injection pool contains chloride as the major anion, there is a pronounced hyperpolarization, with measured resting potentials approaching −150 mV. Blaustein and Goldman (1966) found this to be caused by liquid junction potentials at the interfaces between sucrose and high ionic strength

solutions. The present results are entirely consistent with this picture. If there is a drop in potential upon going from the central pool (ground) to sucrose this has the same effect as making E_{ms} more negative. In turn, this translates into a hyperpolarized value of V_o. To model this influence E_{ms} becomes the sum of E_{ms} and the liquid junction potential. In all of the present work, the hyperpolarizing liquid junction potential was eliminated by using acetate as the major anion. In a few trial experiments chloride-rich solutions were used. This led to the usual hyperpolarized resting potentials but no observable influence on leakage. Sucrose hyperpolarization alters the holding current required to clamp the potential to a given DC level but does not influence the change in current upon a step change in potential.

The La^{3+} Effect

For users of the sucrose gap technique who have been frustrated by short preparation viability and instability, La is an almost magical solution to many problems. At high concentrations La^{3+} has a potent ability to shift active conductance-voltage curves in the depolarizing direction, and it exerts a partial channel blocking action (Takata et al., 1966; Blaustein and Goldman, 1968). When the doping concentration (67 μM in La 10) is added to a high ionic strength central pool solution containing 25 mM calcium, no La^{3+} influence is observed. This was tested in experiments using undoped sucrose where the central pool membrane had no prior exposure to La^{3+}. Switching to a solution containing 67 μM La^{3+} caused no visual change in voltage clamped sodium currents. Thus, exposure of a node to doped sucrose as the axon is pulled through the chamber is not likely to affect voltage clamp currents originating in the node. However, adding La^{3+} to low ionic strength sucrose obviously stabilizes the membrane under sucrose. Some of the stabilizing effect is probably associated with a reduction in surface potential and some with a direct binding to membrane components that somehow require multivalent cations for structural integrity. Just why membranes require calcium or calcium substitutes for their integrity is still not clear (Chizzonite and Zak, 1982), but the practical benefit of doping sucrose with La^{3+} is obvious. As shown in Fig. 6 drift and change over an hour's time are reduced to the slow decay typical of in vitro preparations in general. This will make it easier to study pharmacological influences on channel properties that are slow to develop or slow to decay upon rinsing.

Other Preparations

When the double sucrose gap technique is used on squid axons, the leakage conductance is 10–30 mS cm^{-2} (Moore et al., 1964 *a*; Moore et al., 1964 *b*). Assuming a typical squid axon diameter of 450 μm and a node length of half the axon diameter, this gives a gap leak of 32–95 μS. Computations with the conventional model (using a membrane resistance of 1,000 Ωcm^2) predict a gap leak of only 3.2 μS. Thus the squid axon in sucrose gap, like the lobster axon, exhibits an anomalously high leak. Such a high leak is predicted by the McGuigan-Tsien model by setting R_{ms} to a low value. This strongly suggests that the principles described in this paper are equally applicable to the squid axon, although the lower membrane resistance in squid means that observed properties are probably somewhat less sensitive to events in the sucrose.

The most widespread use of the sucrose gap technique has been to multicellular cardiac muscle preparations where intercellular gap junctions rather than cytoplasmic resistivity control the internal longitudinal resistance. If the junctions close as a result of sucrose treatment, the internal resistance would rise precipitously and there would be a significant change in electrical properties. If doping with lanthanum can prevent closure of gap junctions, by preventing loss of intracellular ions or by a direct influence on junctional permeability, this would make the sucrose gap technique even more attractive for use in voltage clamp studies on cardiac muscle preparations.

We thank Russell McKown for helpful discussion, Andrew Weiner for technical assistance, and Adrienne L. McLean for secretarial assistance.

This work was supported by National Institutes of Health grant NSO9040.

Received for publication 29 October 1982 and in final form 9 March 1983.

REFERENCES

Adelman, W. J. 1956. The effect of external calcium and magnesium depletion on single nerve fibers. *J. Gen. Physiol.* 39:753–772.

Beeler, G. W., and J. A. S. McGuigan. 1978. Voltage clamping of multicellular myocardial preparations: capabilities and limitations of existing methods. *Prog. Biophys. Mol. Biol.* 34:219–254.

Blaustein, M. P., and D. E. Goldman. 1966. Origin of axon membrane hyperpolarization under sucrose-gap. *Biophys. J.* 6:453–470.

Blaustein, M. P., and D. E. Goldman. 1968. The action of certain polyvalent cations on the voltage-clamped lobster axon. *J. Gen. Physiol.* 51:279–291.

Brinley, F. J. 1965. Sodium, potassium and chloride concentrations and fluxes in the isolated giant axon of *Homarus*. *J. Neurophysiol. (Bethesda)*. 28:742–772.

Chizzonite, R. A., and R. Zak. 1982. Calcium-induced cell death: susceptibility of cardiac myocytes is age-dependent. *Science (Wash. DC)*. 213:1508–1511.

Crevey, B. J., G. A. Langer, and J. S. Frank. 1978. Role of Ca^{2+} in maintenance of rabbit myocardial cell membrane structural and functional integrity. *J. Mol. Cell. Cardiol.* 10:1081–1100.

Dalton, J. C. 1958. Effects of external ions on membrane potentials of a lobster giant axon. *J. Gen. Physiol.* 41:529–542.

Govind, C. K., and F. Lang. 1976. Growth of lobster giant axons: correlation between conduction velocity and axon diameter. *J. Comp. Neurol.* 170:421–434.

Huxley, A. F. 1959. Ion movements during nerve activity. *Ann. NY Acad. Sci.* 2:221–246.

Jirounek, P., and R. W. Straub. 1971. The potential distribution and the short-circuiting factor in the sucrose gap. *Biophys. J.* 11:1–10.

Julian, F. J., J. W. Moore, and D. E. Goldman. 1962*a*. Membrane potentials of the lobster giant axon obtained by use of the sucrose-gap technique. *J. Gen. Physiol.* 45:1195–1216.

Julian, F. J., J. W. Moore, and D. E. Goldman. 1962*b*. Current-voltage relations in the lobster giant axon membrane under voltage clamp conditions. *J. Gen. Physiol.* 45:1217–1238.

McGuigan, J. A. S., and R. W. Tsien. 1974. On the cable theory of the double sucrose gap. Appendix to J. A. S. McGuigan. 1974. *J. Physiol.* (*Lond.*). 240:775–806.

McLaughlin, S. G. A., G. Szabo, and G. Eisenman. 1971. Divalent ions and the surface potential of charged phospholipid membranes. *J. Gen. Physiol.* 58:667–687.

Moore, J. W., T. Narahashi, and W. Ulbricht. 1964. Sodium conductance shift in an axon internally perfused with a sucrose and low-potassium solution. *J. Physiol.* (*Lond.*). 172:163–173.

Moore, J. W., W. Ulbricht, and M. Takata. 1964. Effect of ethanol on the sodium and potassium conductances of the squid axon membrane. *J. Gen. Physiol.* 48:279–295.

Muir, A. R. 1967. The effects of divalent cations on the ultrastructure of the perfused rat heart. *J. Anat.* 101:239–261.

New, W., and W. Trautwein. 1972. Inward membrane currents in mammalian myocardium. *Pflugers Arch. Eur. J. Physiol.* 334:1–23.

Oxford, G. S., and J. P. Pooler. 1975. Selective modification of sodium channel gating in lobster axons by 2,4,6-trinitrophenol. Evidence for two inactivation mechanisms. *J. Gen. Physiol.* 66:765–779.

Pooler, J. P., and G. S. Oxford. 1972. Low membrane resistance in sucrose gap—a parallel leakage path. *Biochim. Biophys. Acta.* 255:681–684.

Stampfli, R. 1954. A new method for measuring membrane potentials with external electrodes. *Experientia* (*Basel*). 10:508–509.

Takata, M., W. F. Pickard, J. Y. Lettvin, and J. W. Moore. 1966. Ionic conductance changes in lobster axon membrane when lanthanum is substituted for calcium. *J. Gen. Physiol.* 50:461–471.